REPORT DOCUMENTATION PAGE		*Form Approved* *OMB No. 0704-0188*

1. AGENCY USE ONLY *(Leave blank)*	2. REPORT DATE 6 July 1994	3. REPORT TYPE AND DATES COVERED Scientific Report No. 1

4. TITLE AND SUBTITLE	5. FUNDING NUMBERS
SSUSI Single Sensor Auroral E-layer Algorithm: Functional Description	PE 35160F PR DMSP TA 01 WU AC

6. AUTHOR(S)	
Robert E. Daniell, Jr., William G. Whartenby, & Lincoln D. Brown	Contract F19628-91-C-0103

7. PERFORMING ORGANIZATION NAME(S) AND ADDRESS(ES)	8. PERFORMING ORGANIZATION REPORT NUMBER
Computational Physics, Inc. Suite 202A 240 Bear Hill Road Waltham, MA 02154	

9. SPONSORING / MONITORING AGENCY NAME(S) AND ADDRESS(ES)	10. SPONSORING / MONITORING AGENCY REPORT NUMBER
Phillips Laboratory 29 Randolph Street Hanscom AFB, MA 01731-3010 Contract Manager: Christopher Sherman/GPIM	PL-TR-94-2195

11. SUPPLEMENTARY NOTES

12a. DISTRIBUTION / AVAILABILITY STATEMENT	12b. DISTRIBUTION CODE
APPROVED FOR PUBLIC RELEASE; DISTRIBUTION UNLIMITED	19941205 033

13. ABSTRACT *(Maximum 200 words)*

This report describes the SSUSI single sensor Auroral E-layer algorithm developed by Computational Physics, Inc. for Phillips Laboratory and provided to the Johns Hopkins University Applied Physics Laboratory for incorporation into the operational software for SSUSI. SSUSI is an Ultraviolet Disk and Limb Imager to be flown aboard DMSP satellites for ionospheric and thermospheric remote sensing purposes. The algorithm described here uses the Lyman-α intensity and the intensities in two wavelength bands dominated by the Lyman-Birge-Hopfield band system from molecular nitrogen to estimate the characteristic energy and energy flux of electrons and protons in the auroral region. A simple auroral chemistry model is then used to estimate the peak density and height of the auroral E-layer. Uncertainties in the measured intensities and the algorithm parameters are estimated at each stage of the calculation and an estimate of the uncertainty in the calculated quantities is provided along with the quantities themselves.

14. SUBJECT TERMS			15. NUMBER OF PAGES 40
ionosphere, space environment, remote sensing, space weather, aurora, E-layer			16. PRICE CODE

17. SECURITY CLASSIFICATION OF REPORT Unclassified	18. SECURITY CLASSIFICATION OF THIS PAGE Unclassified	19. SECURITY CLASSIFICATION OF ABSTRACT Unclassified	20. LIMITATION OF ABSTRACT SAR

PL-TR-94-2195

SSUSI Single Sensor Auroral E-layer Algorithm: Functional Description

Robert E. Daniell, Jr
William G. Whartenby
Lincoln D. Brown

DTIC
SELECTED
DEC 1 3 1994
F
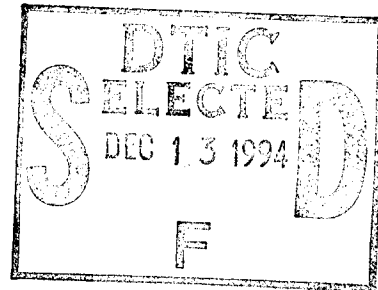
Computational Physics, Inc.
240 Bear Hill Road, Suite 202A
Waltham, MA   02154

6 July 1994

Scientific Report No. 1
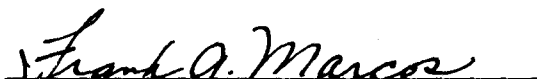
Approved for public release; distribution unlimited

PHILLIPS LABORATORY
Directorate of Geophysics
AIR FORCE MATERIEL COMMAND
HANSCOM AIR FORCE BASE, MA 01731-3010

"This technical report has been reviewed and is approved for publication"

Christopher Sherman
Signature
CHRISTOPHER SHERMAN
Contract Manager

Frank A. Marcos
Signature
for DAVID ANDERSON
Branch Chief

Ken Vickery
Signature
KEN VICKERY
Division Director

This report has been reviewed by the ESC Public Affairs Office (PA) and is releasable to the National Technical Information Service (NTIS).

Qualified requestors may obtain additional copies from the Defense Technical Information Center (DTIC). All others should apply to the National Technical Information Service (NTIS).

If your address has changed, if you wish to be removed from the mailing list, or if the addressee is no longer employed by your organization, please notify PL/TSI, 29 Randolph Road, Hanscom AFB, MA 01731-3010. This will assist us in maintaining a current mailing list.

Do not return copies of this report unless contractual obligation or notices on a specific document requires that it be returned.

SSUSI Single Sensor Auroral E-region Algorithm
Functional Description

Table of Contents

Illustrations

SSUSI Auroral E-region Algorithm

1. Introduction

The SSUSI Auroral E-region algorithm (SSUSIAE) characterizes electron and proton precipitation in the diffuse aurora using select ultraviolet (UV) emissions produced in the E-region of the auroral ionosphere. SSUSIAE also calculates N_mE (the peak electron density of the E-region) and h_mE (the height of the E-region) based on the deduced particle precipitation characteristics.

We have continued to base the algorithm exclusively on Maxwellian incident spectra (appropriate to the continuous aurora) rather than using different spectra for different kinds of aurora. We are aware that discrete auroral arcs are produced by particles with a narrower spectrum (usually represented by Gaussians), but we feel that more work needs to be done on the problem of automatic discrimination of discrete arcs from the continuous aurora. We anticipate that some sort of discrimination will be included in the multi-sensor version of this algorithm.

We have continued to ignore the OI 1356 Å emission in the auroral algorithm. We feel that its usefulness as an operational tool in the single sensor algorithm is quite limited. However, we expect to make use of it in the multi-sensor version of the algorithm.

2. Algorithm Description

SSUSIAE is designed to work with UV images. However, except for the geocoronal background subtraction required for the Lyman α image, and the dayglow background subtraction required for the dayside portion of the auroral oval, it handles each image "pixel by pixel." From the three UV images that it accepts as input, the algorithm produces four images of particle precipitation parameters and two "images" of vertical electron density profile parameters. As delivered, the algorithm assumes that the three images are contained in a single file in which each pixel is tagged by the UT of the measurement, the geographic and geomagnetic location, and the intensities of the three emission features required by the algorithm. The input routine is a separate subprogram and can be easily modified to accommodate any alternative file format.

The three UV emission features used by SSUSIAE are:

1. L_α = Lyman α (1216 Å)
2. LBH1 = LBH 1450 Å band (1400-1500 Å)
3. LBH2 = LBH 1725 Å band (1650-1800 Å)

For each pixel, SSUSIAE determines parameters that describe the incident spectra of precipitating electrons and protons. Since the purpose of this algorithm is to predict behavior in the *diffuse* auroral E-region, the incident particle energy spectra are assumed to have a Maxwellian form that is described by two parameters: the characteristic energy E_0 and the energy flux Q. Therefore, SSUSIAE calculates four precipitation parameters per pixel:

1. $E_{0,e}$, the characteristic energy of the incident electrons
2. Q_e, the energy flux of the incident electrons
3. $E_{0,p}$, the characteristic energy of the incident protons
4. Q_p, the energy flux of the incident protons

Additionally, SSUSIAE determines the ionospheric parameters $N_m E$ and $h_m E$ for each image pixel.

The algorithm also estimates the uncertainty in each of the output parameters due to the uncertainties of the input data and the internal uncertainties of the algorithm itself. Many of the analytic functions that form the auroral algorithm are in the form of power series:

$$\ln[f(a)] = \sum_{n=0}^{N} c_n a^n \tag{1}$$

where f is either the yield of an emission feature or the characteristic energy of a precipitating particle spectrum. a is either an intensity ratio or a characteristic energy. Generally the characteristic energy is first determined from an intensity ratio. Then the yield of an emission feature is determined from the characteristic energy. The yield is used to determine the energy flux. The yield and energy flux may be used to subtract the contribution of one kind of particle

2

(e.g. protons) from the total intensity to reveal the contribution by another kind of particle (e.g., electrons). So the algorithm relies on repeated evaluations of several formulae like Equation (1).

The uncertainty in $\ln(f)$ is estimated from

$$\sigma^2_{\ln(f)} = \sum_{n=0}^{N}\sum_{n'=0}^{N}\sigma^2_{nn'}a^{n+n'} + \sum_{n=0}^{N}\sum_{n'=1}^{N}n'\left(\sigma^2_{na}+\sigma^2_{an'}\right)c_{n'}a^{n+n'-1} + \sigma^2_{aa}\sum_{n=1}^{N}nc_n\sum_{n'=1}^{N}n'\,c_{n'}a^{n+n'-2} \quad (2)$$

where $\sigma^2_{nn'}$ is the covariance of c_n and $c_{n'}$, $\sigma^2_{na}=\sigma^2_{an}$ is the covariance of c_n and a, and σ^2_{aa} is the variance of a. By definition, σ^2_{na} vanishes, so Equation (2) collapses to

$$\sigma^2_{\ln(f)} = \sum_{n=0}^{N}\sum_{n'=0}^{N}\sigma^2_{nn'}a^{n+n'} + \sigma^2_{aa}\sum_{n=1}^{N}\sum_{n'=1}^{N}nn'\,c_nc_{n'}a^{n+n'-2} \quad (3)$$

The $\sigma^2_{nn'}$ are provided by the least squares fitting process that produces the coefficients c_n of Equation (1). When a is an intensity or intensity ratio or other measured quantity, σ^2_{aa} is simply the measurement uncertainty. When a is a derived quantity, its uncertainty is itself estimated using an equation of the form of Equation (3). Finally, the uncertainty in f itself (rather than $\ln f$) is calculated from

$$\sigma_f = \sigma_{\ln(f)}f \quad (4)$$

Note that the accuracy and validity of the above uncertainty estimates depend on the manner in which the series are determined. The actual intensities depend on a number of parameters that are not known, primarily the precise composition of the neutral atmosphere. Although model atmospheres can give reasonable estimates of the neutral composition, the aurora itself modifies the composition, which limits the level of accuracy achievable by a model atmosphere. If the covariances $\sigma^2_{nn'}$ are to be useful as an estimate of the uncertainty in the coefficients due to the variability of "uncontrolled" parameters, the simulated data used to produce Equation (1) must span the natural range of these parameters but not give too much weight to extreme values. Realistically, the uncertainty estimates must be considered crude estimates and should not be over-interpreted.

The top level flow diagram for SSUSIAE appears in Figure 1. The flow diagram for the main part of the algorithm, AURORA, appears in Figure 2. The sections that follow describe each of the major components of SSUSIAE in some detail.

It should be noted that this algorithm was implemented in FORTRAN with the understanding that it would be translated into ADA. Therefore, the coding was done to make the data flow explicit and easily understandable, rather than to take fullest advantage of specific FORTRAN structures.

It should be further noted that this algorithm assumes that the image has been smoothed, geolocated, and rectified. That is, it assumes that

1. any averaging or summing required to reduce the statistical noise to an acceptable level has been done,
2. each pixel is tagged with the correct geographic and geomagnetic coordinates, including solar zenith angle,
3. region boundaries have been determined so that each pixel is also tagged with the region in which it lies, and
4. the intensities have been converted from slant intensities to equivalent vertical intensities.

SSUSIAE
SSUSI Auroral E-layer Algorithm
Top Level Flow Diagram

```
┌──────────────────┐         ╭──────────────────╮
│    READCO:        │◄────────│    disk file:     │
│  read coefficients│         │    algorithm      │
│                   │         │    coefficients   │
└────────┬──────────┘         ╰──────────────────╯
         │
         ▼
┌──────────────────┐         ╭──────────────────╮
│    READGP:        │◄────────│    disk file:     │
│  read geophysical │         │    geophysical    │
│    parameters     │         │    parameters     │
└────────┬──────────┘         ╰──────────────────╯
         │
         ▼
┌──────────────────┐         ╭──────────────────╮
│    READIMG:       │◄────────│    disk file:     │
│read SSUSI image   │         │   SSUSI images    │
│     files         │         │                   │
└────────┬──────────┘         ╰──────────────────╯
         │
         ▼
┌──────────────────┐        ┌──────────────────┐
│   GEOCRNA:        │        │    DAYGLO:        │
│determine geocoronal├──────►│determine the dayglow│
│   background      │        │    background     │
└──────────────────┘        └─────────┬────────┘
                                      │
         ┌────────────────────────────┘
         ▼
┌──────────────────┐
│    AURORA:        │
│executive subprogram│
│ of auroral algorithm│
│   (see Fig. 2)    │
└──────────────────┘
```
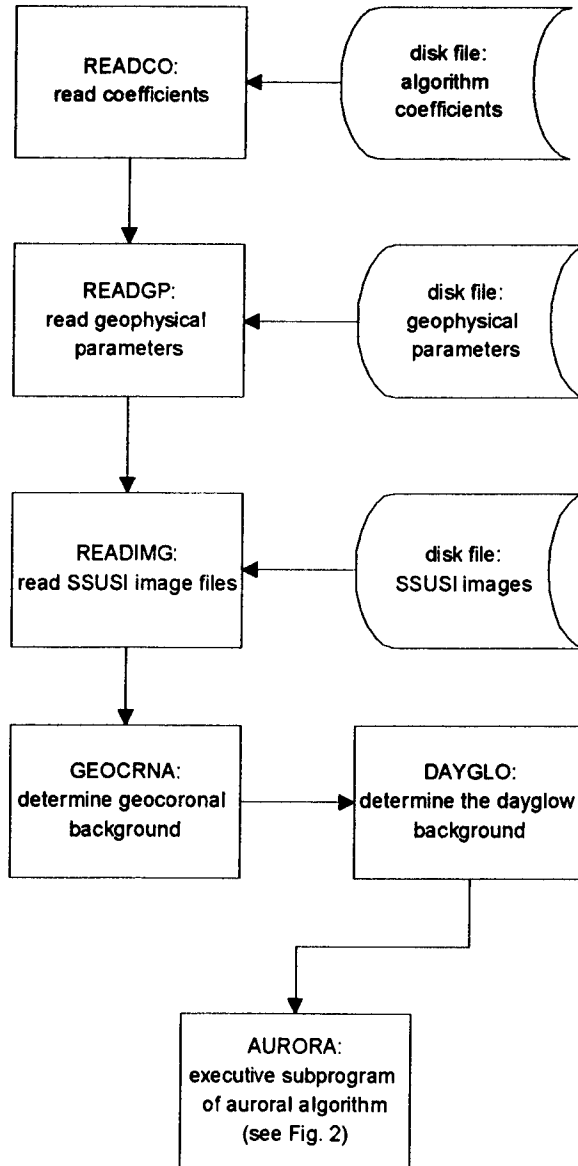
Figure 1. The top level flow diagram for SSUSIAE.

5
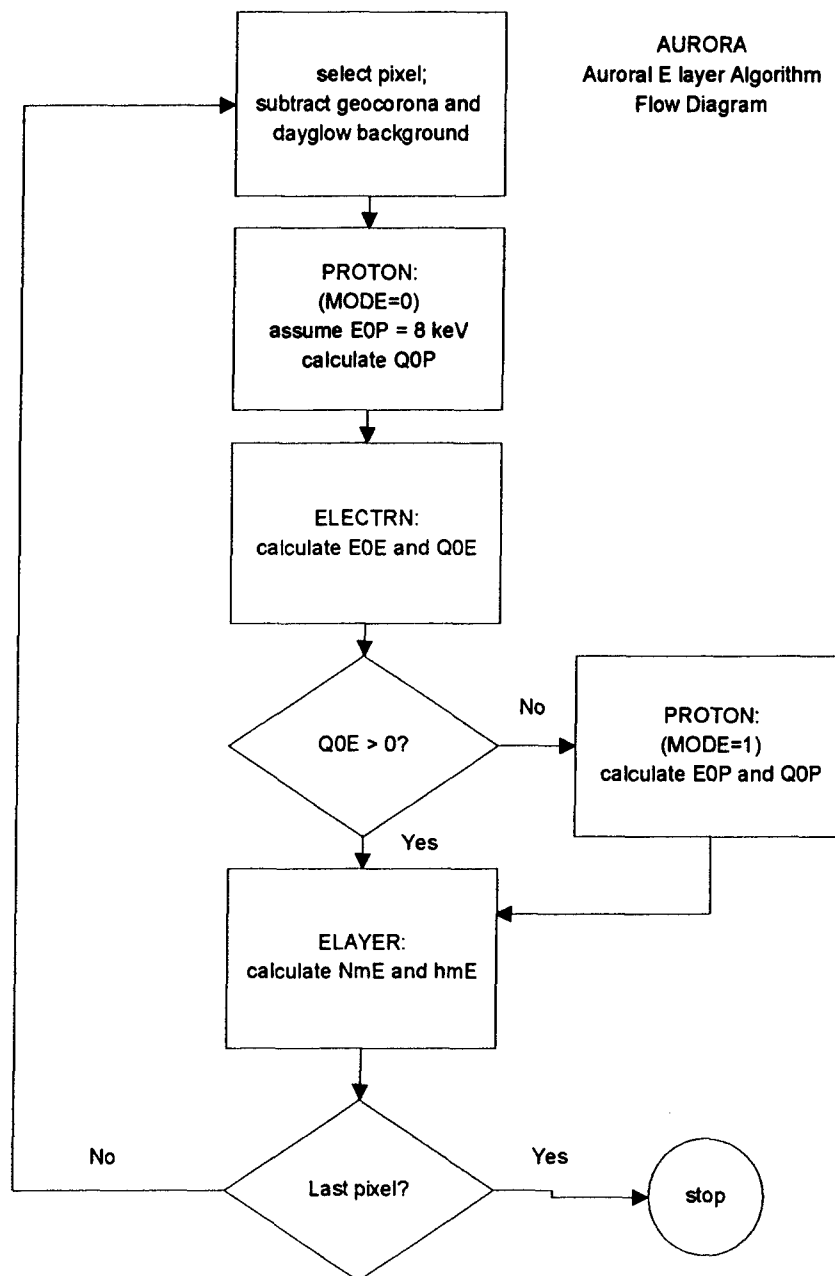
Figure 2. Flow diagram for AURORA and its subsidiary subroutines.

2.1 COMMON /IMAGE/

Because the image data is used unaltered by a number of subroutines, it has been placed in the block COMMON /IMAGE/. The contents of /IMAGE/ conform as closely as possible to the expected contents of the SSUSI Image Mode EDR Data Elements. However, /IMAGE/ represents a subset of the SSUSI EDR. The following variables and arrays are contained in /IMAGE/:

DAY: The day of the year of the image [INTEGER, unitless]

UT: The universal time of the image (presumably the UT of the center of the image) [REAL, hours]

NPIXEL: The actual number of pixels in the image. [INTEGER, unitless]

NROW: The number of rows in the image. [INTEGER, unitless]

NCOL: The number of columns in the image. [INTEGER, unitless]

ROW: The row number of each pixel. [INTEGER ARRAY, unitless]

COLUMN: The column number of each pixel. [INTEGER ARRAY, unitless]

GLAT: The geographic (or geodetic) latitude of each pixel. [REAL ARRAY, degrees]

GLON: The geographic (or geodetic) longitude of each pixel. [REAL ARRAY, degrees]

MLAT: The geomagnetic latitude of each pixel. [REAL ARRAY, degrees]

MLON: The geomagnetic longitude of each pixel. [REAL ARRAY, degrees]

SZA: The solar zenith angle of each pixel. [REAL ARRAY, degrees]

SLT: The solar local time of each pixel. [REAL ARRAY, hours]

REGION: The region flag for each pixel. [INTEGER ARRAY, unitless]

I1216: The Lyman α intensity for each pixel. [REAL ARRAY, Rayleighs]

I1450: The LBH 1 (1400 - 1500 Å) intensity for each pixel. [REAL ARRAY, Rayleighs]

I1725: The LBH 2 (1650 - 1800 Å) intensity for each pixel. [REAL ARRAY, Rayleighs]

C1216: The actual number of counts due to Lyman α for each pixel. [REAL ARRAY, counts]

C1450: The actual number of counts due to LBH 1 for each pixel. [REAL ARRAY, counts]

C1725: The actual number of counts due to LBH 2 for each pixel. [REAL ARRAY, counts]

U1216: The uncertainty in the Lyman α intensity for each pixel. [REAL ARRAY, %]

U1450: The uncertainty in the LBH 1 intensity for each pixel. [REAL ARRAY, %]

U1725: The uncertainty in the LBH 2 intensity for each pixel. [REAL ARRAY, %]

The contents of /IMAGE/ are read from a disk file by READIMG (Section 2.5).

2.2 COMMON /ECOEFF/ and COMMON /PCOEFF/

Because the coefficients in the analytic representations of yield curves, etc., that make up the basic algorithm are read by READCO (Section 2.3) and used only in the subprogram PSEVAL, which is deeply nested, they are also stored in block COMMON. The electron coefficients are stored in /ECOEFF/, while the proton coefficients are stored in /PCOEFF/. The analytic representations and coefficients are described in Section 2.3.

2.3 SUBROUTINE READCO

SUBROUTINE READCO is called from the main program with one argument:

LUN: The logical unit number of the file containing the data that is to be read (input)

READCO reads the coefficients of the analytical models of yield vs. characteristic energy and characteristic energy vs. LBH ratio. These coefficients are used by the FUNCTION subprogram PSEVAL to evaluate the yield curves and other functional relationships used in the algorithm. The coefficients are stored in a common block rather than returned as an argument.

In the current version of the algorithm, the analytical models all have the same form:

$$\ln[f(a)] = \sum_{n=0}^{N} c_n^{(bi)} a^n \tag{5}$$

When f represents a *yield* (the optical intensity produced by an energy flux of $1\,\mathrm{erg\,cm^{-2}\,s^{-1}}$), the argument a is the characteristic energy of the precipitating particles producing the emission (or its inverse). When f represents the characteristic energy of the precipitating particles, the argument a is the ratio of the LBH 1400-1500 Å to LBH 1650-1800 Å band intensities (or its inverse). The identity of the precipitating particles is indicated by the first superscript on the coefficients c: $b = e$ for electrons, and $b = p$ for protons. The second superscript on the coefficients is merely an integer used to distinguish the coefficients of each series. For protons:

$i = 1$ for $Y_{1450}^{(p)}$, the yield of LBH 1400-1500 Å

$i = 2$ for $Y_{1725}^{(p)}$, the yield of LBH 1650-1800 Å

$i = 3$ for $Y_{1216}^{(p)}$, the yield of Lyman α (1216 Å)

$i = 4$ for $E_{0,p}$, the characteristic energy of the incident proton spectrum

For electrons:

$i = 1$ for $Y_{1450}^{(e)}$, the yield of LBH 1400-1500 Å

$i = 2$ for $Y_{1725}^{(e)}$, the yield of LBH 1650-1800 Å

$i = 3$ for $E_{0,e}$, the characteristic energy of the incident proton spectrum

The uncertainties of the calculated quantities are estimated using Equations (3) and (4).

In addition, READCO reads coefficients and parameters for ELAYER, which calculates N_mE and h_mE and their uncertainties. This model is described in Section 2.11.

2.4 SUBROUTINE READGP

SUBROUTINE READGP is called from the main program with five arguments:

F10P7: the solar activity index $F_{10.7}$ [REAL, Solar Flux units]
AP: the magnetic activity index A_p [REAL, unitless]
KP: the magnetic activity index K_p [REAL, unitless]
QEUV: the Q_{EUV} solar activity index determined from the SSUSI daytime algorithm
        [REAL, erg cm^{-2} s^{-1}]
LUN: the logical unit number of the file containing the first three variables [INTEGER]

READGP reads the geophysical parameters from a file. In the operational version, this should be replaced with a call to the appropriate data in the Environmental Database at the Space Forecast Center. However, the Q_{EUV} parameter should be passed in some manner from the Daytime Algorithm. In the current version of this algorithm, these parameters are used only to estimate the solar contribution to the E-layer electron density.

2.5 SUBROUTINE READIMG

SUBROUTINE READIMG is called from the main program with one argument:

LUN: the logical unit number of the file containing the images [INTEGER]

READIMG reads the pixel parameters and stores them in COMMON /IMAGE/ (Section 2.1).
In the operational version, this subroutine must be modified to read image files in the format produced by APL algorithms.

2.6 SUBROUTINE GEOCRNA

SUBROUTINE GEOCRNA is called from the main program with 5 arguments:

A: The constant term in the functional form of the geocoronal background
          [REAL, Rayleighs].
B: The coefficient of the cosine solar zenith angle term in the functional form of
          the geocoronal background [REAL, Rayleighs].

9

AVAR: The variance of A [REAL, Rayleighs^2]
BVAR: The variance of B [REAL, Rayleighs^2]
ABVAR: the covariance of A and B [REAL, Rayleighs^2]

GEOCRNA also has access to the contents of COMMON /IMAGE/.

GEOCRNA does not actually subtract the geocoronal Lyman α background from the Lyman α image, but merely returns coefficients that allow the subtraction to be done later. The algorithm is based on the assumption that the geocoronal background may be represented by the simple functional form

$$I_b = A + B \cos \chi \tag{6}$$

where I_b is the background intensity in Rayleighs and χ is the solar zenith angle. The algorithm assumes that the auroral boundaries have already been identified and that each pixel is flagged so that it can be identified as either *auroral* or *non-auroral*. Only non-auroral pixels are used to determine A and B by means of a straightforward least squares fit. The fitting process produces estimates of the variances of A and B, as well as the covariance of the two with each other, and these are used to estimate the "noise level" of the image. These are returned to the calling program for use in calculating the "noise level," U_{2bck}, as

$$U_{2bck} = 2\sqrt{\sigma_A^2 + \sigma_B^2 \cos^2 \chi + 2\sigma_{AB}^2 \cos \chi} \tag{7}$$

where σ_A^2 is the variance of A, σ_B^2 is the variance of B, and σ_{AB}^2 is the covariance of A and B. (Whenever the difference between the measured intensity and the modeled background intensity is less than the noise level, the difference is set to zero.)

2.7 SUBROUTINE DAYGLO

Like GEOCRNA, SUBROUTINE DAYGLO determines coefficients that allow the subtraction of the dayglow from the two LBH images. It is called from the main program with ten arguments.

A1450: the constant term of the LBH 1400-1500 Å dayglow expression [REAL, Rayleighs]
B1450: the coefficient of the cosine term of the LBH 1400-1500 Å dayglow [REAL, Rayleighs]
VA1450: the variance of A1450 [REAL, Rayleighs^2]
VB1450: the variance of B1450 [REAL, Rayleighs^2]
VC1450: the covariance of A1450 and B1450 [REAL, Rayleighs^2]
A1725: the constant term of the LBH 1650-1725 Å dayglow expression [REAL, Rayleighs]

B1725: the coefficient of the cosine term of the LBH 1650-1725 Å dayglow expression [REAL, Rayleighs]

VA1725: the variance of A1725 [REAL, Rayleighs^2]

VB1725: the variance of B1725 [REAL, Rayleighs^2]

VC1725: the covariance of A1725 and B1725 [REAL, Rayleighs^2]

In addition, DAYGLO has access to the contents of /IMAGE/.

This algorithm is similar to GEOCRNA except that instead of fitting all *non-auroral* pixels, it fits only *day* pixels. The fitting function similar to the one used in GEOCRNA:

$$I_\lambda^{(dayglow)} = A_\lambda + \frac{B_\lambda}{Ch(\chi)} \tag{8}$$

where λ is either 145 nm for LBH1 or 172.5 nm for LBH2, χ is the solar zenith angle, and $Ch(\chi)$ is the Chapman grazing incidence function, which we approximate by [*Rishbeth and Garriott, 1969*]

$$Ch(\chi) \cong \begin{cases} \sqrt{\frac{1}{2}\pi x \sin \chi} \; e^{\frac{1}{2}x\cos^2 \chi} \left[1 - erf\left(\sqrt{\frac{1}{2}x\cos^2 \chi} \right) \right], & \chi < 90° \\ \sqrt{\frac{1}{2}\pi x \sin \chi} \; e^{\frac{1}{2}x\cos^2 \chi} \left[1 + erf\left(\sqrt{\frac{1}{2}x\cos^2 \chi} \right) \right], & \chi \geq 90° \end{cases} \tag{9}$$

where $x = (R_\oplus + z)/H_{N_2}$. We treat x as a constant with a value of 720 (obtained by setting $z = 110$ km and $H_{N_2} = 9$ km). We approximate the error function as [*Abramowitz and Stegun, 1964*]:

$$erf(u) = 1 - \left(a_1 t + a_2 t^2 + a_3 t^3 + a_4 t^4 + a_5 t^5 \right) e^{-u^2} + \varepsilon(u) \tag{10}$$

with

$$t = \frac{1}{1 + pu}$$

and

$p = 0.3275911$	$a_1 = 0.254829592$	$a_2 = -0.284496736$
$a_3 = 1.421413741$	$a_4 = -1.453152027$	$a_5 = 1.061405429$

(For χ less than about 60°, $Ch(\chi)$ is well approximated by $\sec \chi$.)

The variance of $I_\lambda^{(dayglow)}$ is

$$\sigma_\lambda^2 = \sigma_{A_\lambda}^2 + \sigma_{B_\lambda}^2 \cos^2 \chi + 2\sigma_{A_\lambda B_\lambda}^2 \cos \chi \tag{11}$$

where the variances and covariances of A_λ and B_λ are determined by the least squares fitting process.

11

2.8 SUBROUTINE AURORA

SUBROUTINE AURORA is the primary subprogram of the auroral algorithm, it loops over pixels, calling SUBROUTINE PROTON, SUBROUTINE ELECTRN, and SUBROUTINE ELAYER as needed. It is called from the main program with 27 arguments.

A:	the constant term of the geocorona background [REAL, Rayleighs]
B:	the coefficient of the cosine solar zenith angle term of the geocorona background [REAL, Rayleighs]
AVAR:	the variance of A [REAL, Rayleighs^2]
BVAR:	the variance of B [REAL, Rayleighs^2]
ABVAR:	the covariance of A and B [REAL, Rayleighs^2]
A1450:	the constant term of the LBH 1400-1500 Å dayglow expression [REAL, Rayleighs]
B1450:	the coefficient of the cosine term of the LBH 1400-1500 Å dayglow expression [REAL, Rayleighs]
VA1450:	the variance of A1450 [REAL, Rayleighs^2]
VB1450:	the variance of B1450 [REAL, Rayleighs^2]
VC1450:	the covariance of A1450 and B1450 [REAL ARRAY, Rayleighs^2]
A1725:	the constant term of the LBH 1650-1725 Å dayglow expression [REAL, Rayleighs]
B1725:	the coefficient of the cosine term of the LBH 1650-1725 Å dayglow expression [REAL, Rayleighs]
VA1725:	the variance of A1725 [REAL, Rayleighs^2]
VB1725:	the variance of B1725 [REAL ARRAY, Rayleighs^2]
VC1725:	the covariance of A1725 and B1725 [REAL ARRAY, Rayleighs^2]
E0E:	the array containing the deduced electron characteristic energy [REAL ARRAY, keV]
Q0E:	the array containing the deduced electron energy flux [REAL ARRAY, erg cm^{-2} s^{-1}]
E0P:	the array containing the deduced proton characteristic energy [REAL ARRAY, keV]
Q0P:	the array containing the deduced proton energy flux [REAL ARRAY, erg cm^{-2} s^{-1}]
NME:	the array containing the deduced peak E-layer density [REAL ARRAY, cm^{-3}]
HME:	the array containing the deduced E-layer height [REAL ARRAY, km]
UE0E:	the array containing the uncertainty in the deduced electron characteristic energy [REAL ARRAY, keV]
UQ0E:	the array containing the uncertainty in the deduced electron energy flux [REAL ARRAY, erg cm^{-2} s^{-1}]
UE0P:	the array containing the uncertainty in the deduced proton characteristic energy [REAL ARRAY, keV]
UQ0P:	the array containing the uncertainty in the deduced proton energy flux [REAL ARRAY, erg cm^{-2} s^{-1}]

12

UNME: the array containing the uncertainty in the deduced peak E-layer density [REAL ARRAY, cm^{-3}]

UHME: the array containing the uncertainty in the deduced E-layer height (REAL ARRAY, km]

AURORA also has access to the contents of /IMAGE/.

AURORA loops over all pixels. If a pixel is tagged as auroral, then it

(1) subtracts the geocoronal and dayglow backgrounds and estimates the uncertainty of the result,
(2) calls PROTON with MODE=0,
(3) calls ELECTRN, and
(4) *if and only if* Q0E is small enough (Q0E < 0.001 Q0P), it calls PROTON with (MODE=1).

Otherwise, it merely skips the pixel.

The background subtraction and uncertainty estimation proceeds as follows. For the geocorona

$$I_{geocorona} = A + B \cos \chi \tag{12}$$

and

$$\sigma^2_{geocorona} = \sigma^2_A + \sigma^2_B \cos^2 \chi + 2\sigma^2_{AB} \cos \chi \tag{13}$$

The proton contribution to the Lyman α intensity is estimated as

$$I^{(p)}_{1216} = \begin{cases} I_{1216} - I_{geocorona}, & \text{if } I_{1216} > I_{geocorona} + 2\sigma_{geocorona} \\ 0, & \text{otherwise} \end{cases} \tag{14}$$

where I_{1216} is the measured intensity at 121.6 nm.

The uncertainty in $I^{(p)}_{1216}$ is estimated by

$$\sigma^2_{1216,p} = \sigma^2_{1216} + \sigma^2_{geocorona} \tag{15}$$

For the dayglow

$$I^{(dayglow)}_\lambda = A_\lambda + \frac{B_\lambda}{Ch(\chi)} \tag{16}$$

13

where λ is either 145 nm for LBH1 or 172.5 nm for LBH2, χ is the solar zenith angle, and $Ch(\chi)$ is the Chapman grazing incidence function described in Section 2.5 above.

The variance of $I_\lambda^{(dayglow)}$ is

$$\sigma^2_{\lambda,dayglow} = \sigma^2_{A_\lambda} + \sigma^2_{B_\lambda} \cos^2 \chi + 2\sigma^2_{A_\lambda B_\lambda} \cos \chi \qquad (17)$$

As for the geocoronal subtraction, the auroral (proton + electron) contribution to I_λ, the measured intensity at wavelength λ, is estimated by

$$I_\lambda^{(e+p)} = \begin{cases} I_\lambda - I_\lambda^{(dayglow)}, & \text{if } I_\lambda > I_\lambda^{(dayglow)} + 2\sigma_\lambda \\ 0, & \text{otherwise} \end{cases} \qquad (18)$$

The uncertainty in $I_\lambda^{(e+p)}$ is estimated from

$$\sigma^2_{\lambda,e+p} = \sigma^2_\lambda + \sigma^2_{\lambda,dayglow} \qquad (19)$$

2.9 SUBROUTINE PROTON

SUBROUTINE PROTON is called from AURORA with 15 arguments:

I1216: the Lyman α intensity after background subtraction [REAL, Rayleighs]

I1450: the LBH 1 (1400 - 1500 Å) intensities after dayglow subtraction [REAL, Rayleighs]

I1725: the LBH 2 (1650 - 1800 Å) intensities after dayglow subtraction [REAL, Rayleighs]

U1216: the uncertainty in the Lyman α intensity after background subtraction [REAL, Rayleighs]

U1450: the uncertainty in the LBH 1 intensities after dayglow subtraction [REAL, Rayleighs]

U1725: the uncertainty in the LBH 2 intensities after dayglow subtraction [REAL, Rayleighs]

E0E: the characteristic energy of the precipitation electrons. [REAL, keV]
NOTE: If MODE (see below) is 0, then this parameter is unused.

Q0E: the energy flux of precipitating electrons. [REAL, erg cm^{-2} s^{-1}]
NOTE: If MODE is 0, then this parameter is unused.

UE0E: the uncertainty in E0E [REAL, keV]

UQ0E: the uncertainty in Q0E [REAL, erg cm^{-2} s^{-1}]

MODE: an integer variable indicating the "mode" in which PROTON is to calculate the proton precipitation parameters. [INTEGER]

E0P: the characteristic energy of the precipitation protons. [REAL, keV]
NOTE: If MODE is 0, then this parameter is set to 8 keV.

Q0P: the energy flux of precipitating protons. [REAL, erg cm^{-2} s^{-1}]

UE0P: the uncertainty in E0P [REAL, keV]

UQ0P: the uncertainty in Q0P [REAL, erg cm^{-2} s^{-1}]

PROTON operates on a single pixel all of the arguments are scalars. There are two possible modes: MODE = 0 when the electron contribution is unknown, and MODE = 1 when the electron contribution is known.

For MODE = 0, PROTON estimates the incident proton energy flux, Q_p, by assuming that $E_{0,p}$ = 8 keV. The uncertainty in $E_{0,p}$ is set to 4 keV (50% of the assumed $E_{0,p}$).

For MODE = 1, PROTON subtracts the electron contribution to the two LBH bands using E0E and Q0E. It then estimates both $E_{0,p}$ from the ratio of the two LBH bands and Q_p from the Lyman α intensity.

As a practical matter, there is no way to estimate the electron contribution independent of the proton contribution using SSUSI data alone. Therefore, MODE = 1 is used only when the electron contribution is believed to be zero or negligible. The normal calling sequence is

1. Call PROTON with MODE = 0 to get an estimate of the proton flux.
2. Call ELECTRN to get an estimate of the electron flux.
3. *If and only if* the estimate of the electron energy flux is less than 10^{-3} times the proton flux, Call PROTON with MODE = 1 and Q0E = 0.0 to get a refined estimate of the proton energy flux and mean energy.

The proton energy flux is estimated from an expression of the form

$$Q_p\left(d, t, I_{1216}^{(p)}\right) = \frac{I_{1216}^{(p)}}{Y_{1216}^{(p)}} \tag{20}$$

where $Y_{1216}^{(p)}$ is the Lyman α yield of a 1 erg cm^{-2} s^{-1} proton aurora, and

$$I_{1216}^{(p)} = \begin{cases} I_{1216} - I_{1216}^{(geocorona)}, & \text{if } I_{1216} - I_{1216}^{(geocorona)} > U_{2bck} \\ 0, & \text{otherwise} \end{cases} \tag{21}$$

The yield is estimated from the series

$$\ln\left[Y_{1216}^{(p)}\left(E_{0,p}\right)\right] = \sum_{n=0}^{3} c_n^{(p3)} E_{0,p}^n \tag{22}$$

When MODE = 0, $E_{0,p}$ is set to 8 keV. Otherwise (MODE = 1), $E_{0,p}$ is determined from the ratio of the 1400-1500 Å LBH and 1650-1800 Å LBH intensities through an expression of the form

15

$$\ln\left[E_{0,p}\left(R_{LBH}\right)\right] = \sum_{n=0}^{1} c_n^{(p2)} R_{LBH}^n = c_0^{(p2)} + c_1^{(p2)} R_{LBH} \qquad (23)$$

where

$$R_{LBH} = \frac{I_{1450}^{(p)}}{I_{1725}^{(p)}} \qquad (24)$$

and

$$I_\lambda^{(p)} = I_\lambda - I_\lambda^{(dayglow)} - I_\lambda^{(e)} \qquad (25)$$

with λ either 1450 Å or 1725 Å. (The background subtraction is assumed to have been carried out before the call to PROTON)

In MODE = 1, the electron contribution to the two LBH intensities is estimated from expressions of the form

$$I_\lambda^{(e)}\left(E_{0,e}, Q_e\right) = Q_e Y_\lambda^{(e)}\left(E_{0,e}\right)$$

where

$$\ln\left[Y_{1450}^{(e)}\left(E_{0,e}\right)\right] = \sum_{n=0}^{3} c_n^{(e1)} E_{0,e}^n \qquad (26)$$

$$\ln\left[Y_{1725}^{(e)}\left(E_{0,e}\right)\right] = \sum_{n=0}^{3} c_n^{(e2)} E_{0,e}^n \qquad (27)$$

Of course, in normal usage Q_e will be zero and both $I_{1450}^{(e)}$ and $I_{1725}^{(e)}$ will vanish. As delivered, the FORTRAN code tests Q0E, and if it is exactly zero, the electron contribution is set to zero without evaluating the above series.

2.10 SUBROUTINE ELECTRN

SUBROUTINE ELECTRN is called from AURORA with 10 arguments:

I1450:   the summed intensities in the LBH 1 wavelength range (1400-1500 Å) [REAL, Rayleighs]

I1725:   the summed intensities in the LBH 2 wavelength range (1650-1800 Å) [REAL, Rayleighs]

C1450:   the actual number of counts due to the LBH 1 intensity [INTEGER, unitless]

C1725:   the actual number of counts due to the LBH 2 intensity [INTEGER, unitless]

E0P: the characteristic energy of the precipitation protons. [REAL, keV]

16

QOP: the energy flux of precipitating protons. [REAL, erg cm^{-2} s^{-1}]

EOE: the characteristic energy of the precipitation electrons. [REAL, keV]

QOE: the energy flux of precipitating electrons. [REAL, erg cm^{-2} s^{-1}]

UEOE: the uncertainty in the characteristic energy of the precipitation electrons. [REAL, keV]

UQOE: the uncertainty in the energy flux of precipitating electrons. [REAL, erg cm^{-2} s^{-1}]

Like PROTON, ELECTRN operates on a single pixel, so all of the arguments are scalars.

ELECTRN calculates the energy flux and characteristic energy from the two LBH bands after subtracting the proton contribution. If the proton energy flux Q_p is non-zero, ELECTRN calls the FUNCTION subprogram PSEVAL to estimate the proton contribution:

$$I_\lambda^{(p)}\left(E_{0,p}, Q_p\right) = Q_p Y_\lambda^{(p)}\left(E_{0,p}\right)$$

with

$$\ln\left[Y_{1450}^{(p)}\left(E_{0,p}\right)\right] = \sum_{n=0}^{3} c_n^{(p1)} E_{0,p}^n \tag{28}$$

$$\ln\left[Y_{1725}^{(p)}\left(E_{0,p}\right)\right] = \sum_{n=0}^{3} c_n^{(p2)} E_{0,p}^n \tag{29}$$

If the estimated proton contribution is greater than or equal to the observed intensity of either LBH feature, the electron contribution is assumed to vanish. Otherwise, the electron contribution is just the difference between the observed intensity and the estimated proton contribution:

$$I_{1450}^{(e)} = \begin{cases} 0 & \text{if } I_{1450}^{(p)} \geq I_{1450} \\ I_{1450} - I_{1450}^{(p)} & \text{if } I_{1450}^{(p)} < I_{1450} \end{cases} \tag{30}$$

$$I_{1725}^{(e)} = \begin{cases} 0 & \text{if } I_{1725}^{(p)} \geq I_{1725} \\ I_{1450} - I_{1450}^{(p)} & \text{if } I_{1725}^{(p)} < I_{1725} \end{cases} \tag{31}$$

If the estimated electron contribution to *either* LBH feature is zero, then the electron energy flux is also set to zero, and the characteristic energy is set to a minimum value (500 eV).

The calculation of electron precipitation parameters uses the following relationship between characteristic energy, $E_{0,e}$, and the ratio of the two intensities $I_{1450}^{(e)}$ and $I_{1725}^{(e)}$:

17

$$\ln\left[E_{0,e}\left(R_{LBH}^{(e)}\right)\right] = \sum_{n=0}^{3} c_n^{(e3)}\left(R_{LBH}^{(e)}\right)^n \qquad (32)$$

where

$$R_{LBH}^{(e)} = \frac{I_{1450}^{(e)}}{I_{1725}^{(e)}} \qquad (33)$$

Once $E_{0,e}$ has been determined, the energy flux is estimated in the following manner:

$$\ln\left[Y_{1450}^{(e)}\left(E_{0,e}\right)\right] = \sum_{n=0}^{3} c_n^{(e1)} E_{0,e}^n \qquad (34)$$

$$\ln\left[Y_{1725}^{(e)}\left(E_{0,e}\right)\right] = \sum_{n=0}^{3} c_n^{(e2)} E_{0,e}^n \qquad (35)$$

give the yields of the two LBH bands for an electron energy flux of 1 erg cm^{-2} s^{-1}. The ratio of the observed intensity to the yield gives the energy flux:

$$Q_e^{(1450)} = \frac{I_{1450}^{(e)}}{Y_{1450}^{(e)}} \qquad (36)$$

$$Q_e^{(1725)} = \frac{I_{1725}^{(e)}}{Y_{1725}^{(e)}} \qquad (37)$$

Since it is likely that $Q_e^{(1450)}$ and $Q_e^{(1725)}$ will differ, ELECTRN returns the value determined from the feature with the *largest counting rate*. That is

$$Q_e = \begin{cases} Q_e^{(1450)}, & \text{if } C_{1450} \geq C_{1725} \\ Q_e^{(1725)}, & \text{if } C_{1450} < C_{1725} \end{cases} \qquad (38)$$

so that Q_e is determined from the feature that has the lowest uncertainty due to counting statistics.

18

2.11 SUBROUTINE ELAYER

SUBROUTINE ELAYER is called from the main program with 15 arguments:

SZA: solar zenith angle [REAL, degrees]

E0E: the characteristic energy of the precipitating electrons [REAL, keV]

Q0E: the energy flux of the precipitating electrons [REAL, erg cm^{-2} s^{-1}]

E0P: the characteristic energy of the precipitating protons [REAL, keV]

Q0P: the energy flux of the precipitating protons [REAL, erg cm^{-2} s^{-1}]

QEUV: the solar energy flux determined by the daytime algorithm [REAL, erg cm^{-2} s^{-1}]

UE0E: the uncertainty in the characteristic energy of the precipitating electrons [REAL, keV]

UQ0E: the uncertainty in the energy flux of the precipitating electrons [REAL, erg cm^{-2} s^{-1}]

UE0P: the uncertainty in the characteristic energies of the precipitating protons [REAL, keV]

UQ0P: the uncertainty in the energy fluxes of the precipitating protons [REAL, erg cm^{-2} s^{-1}]

UQEUV: the uncertainty in the solar activity index determined by the daytime algorithm [REAL, erg cm^{-2} s^{-1}]

NME: the electron density at the peak of the E-layer [REAL, cm^{-3}]

HME: the height of the peak of the E-layer [REAL, km]

UNME: the uncertainty in the peak electron density [REAL, cm^{-3}]

UHME: the uncertainty in the height of the peak [REAL, km]

Like PROTON and ELECTRN, ELAYER operates on one pixel at a time, so all of the arguments are scalars.

The first step is the determination of the height of the peak ionization due to the two auroral ionization sources (electrons and protons):

$$\log_{10} h_m^{(b)}\left(E_{0,b}\right) = \beta_0^{(b)} - \beta_1^{(b)} \log_{10}\left(\frac{E_{0,b}}{E_{ref}^{(b)}}\right), \qquad b = e, p \qquad (39)$$

where $E_{ref}^{(e)} = 1$ keV and $E_{ref}^{(p)} = 4$ keV. The second step is the determination of the peak production rate for the auroral ionization sources for an incident flux of 1 erg cm^{-2} s^{-1}:

$$\log_{10}\left(\frac{p_m^{(b)}\left(E_{0,b}\right)}{p_m^{(b)}\left(E_{ref}^{(b)}\right)}\right) = \sum_{n=1}^{2} \gamma_n^{(b)}\left[\log_{10}\left(\frac{E_{0,b}}{E_{ref}^{(b)}}\right)\right]^n \qquad b = e, p \qquad (40)$$

The next step is the representation of all three production rate profiles by Chapman layers. We first define a generalized Chapman function $S(u,\psi)$ as

$$S(u,\psi) = \exp\left[1 - u - e^{-u}\mathrm{Ch}(\psi)\right] \qquad (41)$$

where $\mathrm{Ch}(\psi)$ is the Chapman grazing incidence function described in Section 2.5. We write

$$p_i^{(b)}(z;E_{0,b},Q_b) = \frac{Q_b}{1\ \mathrm{erg\ cm^{-2}\ s^{-1}}}\, p_m^{(b)}(E_{0,b})S(u_b,0) \qquad b = e,p \qquad (42)$$

for protons and electrons, and

$$p_i^{(EUV)}(z;Q_{EUV},\chi) = \frac{Q_{EUV}}{1\ \mathrm{erg\ cm^{-2}\ s^{-1}}}\, p_m^{(EUV)}(0)S(u_{EUV},\chi) \qquad (43)$$

for photoionization. In the above expressions

$$u_b = \frac{z - h_m^{(b)}}{H_b} \qquad b = e,p \qquad (44)$$

and

$$u_{EUV} = \frac{z - h_0}{H_n} \qquad (45)$$

For protons and electrons, $h_m^{(b)}$ depends on the characteristic energy, $E_{0,b}$, and is given by Equations (33) and (32), respectively. For photoionization, h_0 is just the height of the peak E-layer ionization at the subsolar point (~108 km), and H_n is just the neutral scale height in the E region (~9 km). For protons and electrons, determining H_b requires a little more effort.

First we note that although the column ionization, $Q_i^{(b)}$, is independent of $E_{0,b}$, the peak ionization, $p_m^{(b)}$, is not. This implies that the *shape* of the ionization profile changes with characteristic energy. In the Chapman function, the shape is controlled by the scale height, H_b, which may be determined in the following manner.

$$Q_i^{(b)} = \int_0^\infty p_i^{(b)}(z)\, dz \quad \approx \quad \frac{H_b Q_b p_m^{(b)}}{1\ \mathrm{erg\ cm^{-2}\ s^{-1}}}\int_{-\infty}^\infty S(u_b,0)\, du_b \qquad (46)$$

Since

$$\int_{-\infty}^\infty S(u,\psi)\, du = e\int_0^\infty e^{-w\mathrm{Ch}(\psi)}\, dw = \frac{e}{\mathrm{Ch}(\psi)} \qquad (47)$$

20

(where e is the base of the natural logarithms, *not* the charge on an electron), we have

$$Q_i^{(b)} \approx \frac{eQ_bH_bp_m^{(b)}}{1 \text{ erg cm}^{-2}\text{ s}^{-1}} \tag{48}$$

or

$$H_b(E_{0,b}) = \frac{1 \text{ erg cm}^{-2}\text{ s}^{-1}}{Q_b} \frac{Q_i^{(b)}}{ep_m^{(b)}(E_{0,b})} \tag{49}$$

For electrons and protons the total *column* ionization rate $Q_i^{(b)}$ in cm^{-2} s^{-1} is related to the incident energy flux of that species Q_b in erg cm^{-2} s^{-1} by

$$Q_i^{(b)} = \rho_b Q_b \tag{50}$$

The proportionality constant ρ_b includes the conversion from erg to eV and the mean "eV per ion pair":

$$\rho_e \approx \frac{1}{43.73 \text{ ev / ion pair} \times 1.6022 \times 10^{-12} \text{ erg / eV}} \approx 1.427 \times 10^{10} \text{ ion pairs / erg}$$

$$\rho_p \approx \frac{1}{27 \text{ ev / ion pair} \times 1.6022 \times 10^{-12} \text{ erg / eV}} \approx 2.3 \times 10^{10} \text{ ion pairs / erg}$$

The "eV per ion pair" for electrons differs from the traditional "35 eV per ion pair" because a significant fraction of the incident electron flux is backscattered out of the atmosphere before it can do any appreciable ionization. H_b is be determined from

$$H_b(E_{0,b}) = \frac{\rho_b \times (1 \text{ erg cm}^{-2}\text{ s}^{-1})}{ep_m^{(b)}(E_{0,b})} \tag{51}$$

The altitude distribution of ionization is now completely specified for all three ionization sources.

The composite electron density profile is calculated using an effective recombination rate, $\alpha(z)$, which is a function of altitude:

$$n_e(z) = \sqrt{\frac{p_i^{(e)}(z) + p_i^{(p)}(z) + p_i^{(EUV)}(z)}{\alpha(z)}} \tag{52}$$

where $n_e(z)$ is the electron density. By squaring both sides of Equation (52) and taking a derivative with respect to z, one may obtain an condition for the maximum electron density:

21

$$\alpha(z)\sum_b \frac{\partial}{\partial z} p_i^{(b)}(z) - \frac{\partial \alpha}{\partial z} \sum_b p_i^{(b)}(z) = 0 \tag{53}$$

or more simply

$$\frac{1}{p_i}\frac{\partial p_i}{\partial z} = \frac{1}{\alpha}\frac{\partial \alpha}{\partial z} \tag{54}$$

where

$$p_i(z) = \sum_b p_i^{(b)}(z) \tag{55}$$

A somewhat crude but serviceable model for $\alpha(z)$ is

$$\alpha(z) = \begin{cases} \alpha_0, & z \le z_\alpha \\ \alpha_0 \exp\left(-\dfrac{z-z_\alpha}{H_\alpha}\right), & z > z_\alpha \end{cases} \tag{56}$$

Consequently, if $z < z_\alpha$, $h_m E$ is the same as the height, h_m, of the peak in the total ionization, p_i. In general, $h_m E$ is determined by

$$\frac{1}{p_i}\frac{\partial p_i}{\partial z} = \begin{cases} 0, & h_m \le z_\alpha \\ -\dfrac{1}{H_\alpha}, & h_m > z_\alpha \end{cases} \tag{57}$$

Unfortunately, it is not possible to derive an expression for $h_m E$ in closed form unless a single ionization source dominates. In that case

$$\frac{1}{p_i^{(b)}}\frac{\partial p_i^{(b)}}{\partial z} = \frac{1}{H_b}\frac{1}{S}\frac{\partial S(u_b,0)}{\partial u_b} = -\frac{1-e^{-u_b}}{H_b} \quad \text{(single ionization source)} \tag{58}$$

From Equation (57)

$$h_m E = \begin{cases} h_m^{(b)}, & h_m^{(b)} \le z_\alpha \\ h_m^{(b)} - H_b \ln\left(1+\dfrac{H_b}{H_\alpha}\right), & h_m^{(b)} > z_\alpha \end{cases} \quad \text{(single ionization source)} \tag{59}$$

When two or more of the ionization sources produce comparable ionization rates, $h_m E$ must be determined using some sort of numerical root finding algorithm. We have decided to use the simplest such algorithm: simply tabulate $n_e(z)$ between 90 and 160 km at $\Delta z = 5$ km intervals and find the largest "internal" maximum. (Specifically, we reject a maximum at the ends of the

22

interval.) If there is no internal maximum, then we set $h_m E$ to 110 km. Although this method is rather crude, it has the virtue of requiring only 14 evaluations of $n_e(z)$. Given the unpredictable and variable nature of the auroral EDP in the E-layer, there is no guarantee that a more sophisticated root finding algorithm would converge in a reasonable number of iterations. Using the simple method, the uncertainty in $h_m E$ is no more than ± 2.5 km ($= \frac{\Delta z}{2}$) unless no internal maximum is found. In that case, however, the auroral contribution to the E-layer must be unimportant, so the uncertainty in $h_m E$ is also unimportant.

Once $h_m E$ has been determined, $N_m E$ is calculated from

$$N_m E = \sqrt{\frac{\sum_b p_i^{(b)}(h_m E)}{\alpha(h_m E)}} = \sqrt{\frac{p(h_m E)}{\alpha(h_m E)}} \tag{60}$$

where $p(z) = \sum_b p_i^{(b)}(z)$ is the total ionization rate at altitude z.

Because of the inherent nonlinearity of these formulae, error analysis for $N_m E$ and $h_m E$ is quite complicated. As a practical matter, we assume that the uncertainty in $h_m E$ calculated from Equation (57) is *no more* than the error in $h_m E$ determined by the tabulation method above. Then a conservative estimate of the uncertainty in $h_m E$ is $\sqrt{2} \frac{\Delta z}{2} = 3.5$ km, and the uncertainty in $N_m E \equiv n_e(h_m E)$ is simply

$$\frac{\sigma_{N_m E}}{N_m E} = \frac{1}{2} \sqrt{\frac{\sigma_p^2}{p^2} + \frac{\sigma_\alpha^2}{\alpha^2}} \tag{61}$$

where we have assumed that the errors in p and α uncorrelated. However, this does not take into account the error in $N_m E$ due to errors in $h_m E$. These are hard to estimate in this calculation method, but we will assume that they are no larger than the uncertainty estimate of Equation (61). In that case, a conservative estimate of the uncertainty in $N_m E$ is

$$\frac{\sigma_{N_m E}}{N_m E} = \frac{\sqrt{2}}{2} \sqrt{\frac{\sigma_p^2}{p^2} + \frac{\sigma_\alpha^2}{\alpha^2}} \tag{62}$$

The uncertainty in p may be estimated from

$$\sigma_p^2 = \sum_b \sigma_{p_i^{(b)}}^2 \tag{63}$$

where the uncertainties in $p_i^{(b)}$ are to be evaluated at $z = h_m E$. These uncertainties depend on the uncertainty in the Chapman function:

$$\frac{\sigma_S^2}{S^2} = \left[e^{-u}\mathrm{Ch}(\chi) - 1\right]^2 \sigma_u^2 \tag{64}$$

with

$$\sigma_u^2 = \frac{\sigma_h^2}{H^2} + \left(\frac{z-h}{H}\right)^2 \frac{\sigma_H^2}{H^2} \tag{65}$$

Similarly, the uncertainty in α may be estimated from

$$\frac{\sigma_\alpha^2}{\alpha^2} = \begin{cases} \dfrac{\sigma_{\alpha_0}^2}{\alpha_0^2}, & z \le z_\alpha \\[3mm] \dfrac{\sigma_{\alpha_0}^2}{\alpha_0^2} + \dfrac{\sigma_{z_\alpha}^2}{H_\alpha^2} + \dfrac{\sigma_{H_\alpha}^2}{H_\alpha^2}\left(\dfrac{z - z_\alpha}{H_\alpha}\right)^2, & z > z_\alpha \end{cases} \tag{66}$$

where the α parameters are assumed to be uncorrelated.

SSUSIAE evaluates uncertainties in each quantity as it is calculated and passes the estimated uncertainty to the next subprogram that needs it. For mathematical completeness, an error analysis giving the uncertainties in $N_m E$ and $h_m E$ in terms of each *primitive* parameter is provided by the Appendix.

2.12 SUBROUTINE WIMAGE

SUBROUTINE WIMAGE is called from the main program with 14 arguments:

NPIXEL: The number of pixels in the image [INTEGER]

E0E: the array that contains the characteristic energies of the precipitating electrons as deduced from the image intensities [REAL ARRAY(NPIXEL), keV]

Q0E: the array that contains the energy fluxes of the precipitation electrons as deduced from the image intensities [REAL ARRAY(NPIXEL), erg cm^{-2} s^{-1}]

E0P: the array that contains the characteristic energies of the precipitating protons as deduced from the image intensities [REAL ARRAY(NPIXEL), keV]

Q0P: the array that contains the energy fluxes of the precipitation protons as deduced from the image intensities [REAL ARRAY(NPIXEL), erg cm^{-2} s^{-1}]

NME: the array that contains the peak electron density of the E layer (N_mE) as deduced from E0E, Q0E, E0P, and Q0E [REAL ARRAY, cm^{-3}]

HME: the array that contains the height of the E-layer [REAL ARRAY, km]

UE0E: the array that contains the uncertainties in the characteristic energies of the precipitating electrons [REAL ARRAY(NPIXEL), keV]

UQ0E: the array that contains the uncertainties in the energy fluxes of the precipitation electrons [REAL ARRAY(NPIXEL), erg cm^{-2} s^{-1}]

UE0P: the array that contains the uncertainties in the characteristic energies of the precipitating protons [REAL ARRAY(NPIXEL), keV]

UQ0P: the array that contains the uncertainties in the energy fluxes of the precipitation protons [REAL ARRAY(NPIXEL), erg cm^{-2} s^{-1}]

UNME: the array that contains the uncertainties in the peak electron density of the E layer (N_mE) [REAL ARRAY, cm^{-3}]

UHME: the array that contains the uncertainties in the height of the E-layer [REAL ARRAY, km]

LUN: the logical unit number of the file where the "image" is to be written.

WIMAGE writes an "image" file in the same format as the original image file except that precipitation parameters ($E_{0,e}$, Q_e, $E_{0,p}$, Q_p, N_mE, and h_mE) and their estimated uncertainties, rather than intensities, are being stored.

WIMAGE is provided solely to allow AURORA to operate as a stand-alone algorithm. We assume that the final package of SSUSI algorithms will have its own I/O module(s) and will dispense with WIMAGE.

APPENDIX: $h_m E$ and $N_m E$ **error propagation analysis in terms of primitive variables**

Both $h_m E$ and $N_m E$ depend on six "arguments": Q_e, Q_p, Q_{EUV}, $E_{0,e}$, $E_{0,p}$, and χ. (In the following error propagation analysis, the uncertainty in χ is assumed to be negligible.) In addition, both depend on a number of other parameters determined by fitting the results of computer modeling with analytic functions. These parameters are

Parameter	Description	Equation(s)
$\beta_n^{(b)}$, $n=0,1,2,3$; $b=e,p$	coefficients in $h_m^{(b)}\left(E_{0,b}\right)$	(39)
h_0	height of peak photoionization at $\chi=0$	(43)
H_n	neutral scale height at $h_m E$	(43)
$\gamma_n^{(b)}$, $n=0,1,2$; $b=e,p$	coefficients in $p_i^{(b)}\left(E_{0,b}\right)$	(40)
$p_m^{(b)}\left(E_{ref}^{(b)}\right)$, $b=e,p$	peak impact ionization rate at the reference energy of $E_{ref}^{(b)}$ (sometimes denoted by $p_{m,ref}^{(b)}$)	(40)
$p_m^{(EUV)}(0)$	peak photoionization at $\chi=0$ (sometimes denoted by $p_{m,0}^{(EUV)}$)	(43)
ρ_b, $b=e,p$	proportionality constant between $Q_i^{(b)}$ and Q_b	after (50)
z_α	the altitude at which $\alpha(z)$ changes from constant to and exponential function	(56)
α_0	$\alpha(z_\alpha)$	(56)
H_α	the scale height of $\alpha(z)$ for $z > z_\alpha$	(56)

The general equation for calculating the uncertainties of $h_m E$ and $N_m E$ are derived here. Explicit expressions in terms of the above parameters follow the general equations.

Both quantities may be thought of as functions of the form

$$f\left(Q_e, Q_p, Q_{EUV}, E_{0,e}, E_{0,p}, \chi; \mathbf{a}\right)$$

where $\mathbf{a}$ is a vector whose elements are all the parameters used in the E layer model, including $\beta_n^{(e)}$, $\beta_n^{(p)}$, $\gamma_n^{(e)}$, $\gamma_n^{(p)}$, $p_m^{(EUV)}(0)$, h_0, H_n, ρ_e, ρ_p, α_0, and z_α. The uncertainty in f may be estimated as [*Bevington and Robinson*, 1992]

$$\sigma_f^2 = \sigma_{Q_e}^2 \left(\frac{\partial f}{\partial Q_e}\right)^2 + \sigma_{Q_p}^2 \left(\frac{\partial f}{\partial Q_p}\right)^2 + \sigma_{Q_{EUV}}^2 \left(\frac{\partial f}{\partial Q_{EUV}}\right)^2 + \sigma_{E_{0,e}}^2 \left(\frac{\partial f}{\partial E_{0,e}}\right)^2 + \sigma_{E_{0,p}}^2 \left(\frac{\partial f}{\partial E_{0,p}}\right)^2$$

$$+ \sum_m \sum_{m'} \sigma_{a_m a_{m'}}^2 \left(\frac{\partial f}{\partial a_m}\right)\left(\frac{\partial f}{\partial a_{m'}}\right)$$

(A1)

where we have assumed that the uncertainty in χ is negligible and that the six arguments are uncorrelated with each other and with the parameters $\mathbf{a}$. Of course, many of the parameters are also uncorrelated with other parameters, so the covariance matrix $\sigma^2_{p_m p_{m'}}$ has many zero elements. It must also be remembered that $N_m E$ depends explicitly on $h_m E$, so the partial derivatives with respect to the arguments and parameters must include the implicit dependences represented by $h_m E$.

If $h_m E$ were determined numerically from Equation (57), the partial derivatives would have to be calculated implicitly. Let

$$g(Q_e, Q_p, Q_{EUV}, E_{0,e}, E_{0,p}, \chi, z; \mathbf{a}) = \frac{\partial p_i}{\partial z} + \frac{p_i}{H_\alpha} \tag{A2}$$

so that $h_m E$ is determined implicitly by

$$g(Q_e, Q_p, Q_{EUV}, E_{0,e}, E_{0,p}, \chi, h_m E; \mathbf{a}) = 0 \tag{A3}$$

The partial derivatives required for the error propagation analysis are obtained as follows.

$$\frac{dg}{db_k} = \frac{\partial g}{\partial b_k} + \frac{\partial g}{\partial h_m E} \frac{\partial h_m E}{\partial b_k} = 0 \tag{A4}$$

or

$$\frac{\partial h_m E}{\partial b_k} = -\left(\frac{\partial g}{\partial h_m E}\right)^{-1} \frac{\partial g}{\partial b_k} \tag{A5}$$

where b_k can be any of the arguments (Q, E, etc.) as well as any parameters represented by $\mathbf{a}$. Taking into account the definition of g, we may obtain

$$\frac{\partial h_m E}{\partial b_k} = -\frac{\left[\frac{\partial^2 p_i}{\partial b_k \partial z} + \frac{1}{H_\alpha} \frac{\partial p_i}{\partial b_k}\right]_{z=h_m E}}{\left[\frac{\partial^2 p_i}{\partial z^2}\bigg|_{z=h_m E} + \frac{1}{H_\alpha} \frac{\partial p_i}{\partial z}\bigg|_{z=h_m E}\right]} \tag{A6}$$

which applies to all arguments and to all parameters used in calculating $p_i(z)$ – that is all parameters except α_0, z_α, and H_α. Explicit expressions for the partial derivatives in Equation (A6) are given below, as are the partial derivatives with respect to the three $\alpha(z)$ parameters.

The derivatives required for the N_mE error propagation analysis are more straightforward:

$$\frac{\partial N_mE}{\partial b_k} = \frac{1}{2N_mE} \frac{\alpha(h_mE)\frac{\partial p_i}{\partial b_k}\Big|_{z=h_mE} - p_i(h_mE)\frac{\partial \alpha}{\partial b_k}\Big|_{z=h_mE} + \left(\frac{1}{\alpha(h_mE)}\frac{\partial p_i}{\partial z}\Big|_{z=h_mE} - \frac{p_i(h_mE)}{\alpha^2(h_mE)}\frac{\partial \alpha}{\partial z}\Big|_{z=h_mE}\right)\frac{\partial h_mE}{\partial b_k}}{\alpha^2(h_mE)}$$

(A7)

or

$$\frac{\partial N_mE}{\partial b_k} = \tfrac{1}{2}N_mE\left[\left(\frac{1}{p_i}\frac{\partial p_i}{\partial b_k} - \frac{1}{\alpha}\frac{\partial \alpha}{\partial b_k}\right)_{z=h_mE} + \left(\frac{1}{p_i}\frac{\partial p_i}{\partial z} - \frac{1}{\alpha}\frac{\partial \alpha}{\partial z}\right)_{z=h_mE}\frac{\partial h_mE}{\partial b_k}\right]$$

However, from Equation (54) we see that the second term in the square brackets vanishes at $z = h_mE$ so the final result is

$$\frac{\partial N_mE}{\partial b_k} = \tfrac{1}{2}N_mE\left[\left(\frac{1}{p_i}\frac{\partial p_i}{\partial b_k} - \frac{1}{\alpha}\frac{\partial \alpha}{\partial b_k}\right)_{z=h_mE}\right]$$

(A8)

The partial derivatives needed for equation (A8) are given below. N_mE is also an explicit function of $\alpha(z)$ and its parameters, α_0, z_α, and H_α. These partial derivatives are also given below.

The explicit expression for the uncertainty defined by Equation (A1), taking into account uncorrelated parameters, is:

$$\sigma_f^2 = \sigma_{Q_e}^2\left(\frac{\partial f}{\partial Q_e}\right)^2 + \sigma_{Q_p}^2\left(\frac{\partial f}{\partial Q_p}\right)^2 + \sigma_{Q_{EUV}}^2\left(\frac{\partial f}{\partial Q_{EUV}}\right)^2 + \sigma_{E_{0,e}}^2\left(\frac{\partial f}{\partial E_{0,e}}\right)^2 + \sigma_{E_{0,p}}^2\left(\frac{\partial f}{\partial E_{0,p}}\right)^2$$

$$+ \sum_{n=0}^{3}\sum_{n'=0}^{3}\sigma_{\beta_n^{(e)}\beta_{n'}^{(e)}}^2\left(\frac{\partial f}{\partial \beta_n^{(e)}}\right)\left(\frac{\partial f}{\partial \beta_{n'}^{(e)}}\right) + \sum_{n=0}^{3}\sum_{n'=0}^{3}\sigma_{\beta_n^{(p)}\beta_{n'}^{(p)}}^2\left(\frac{\partial f}{\partial \beta_n^{(p)}}\right)\left(\frac{\partial f}{\partial \beta_{n'}^{(p)}}\right) + \sigma_{h_0}^2\left(\frac{\partial f}{\partial h_0}\right)^2 + \sigma_{H_n}^2\left(\frac{\partial f}{\partial H_n}\right)^2$$

(A9)

$$+ \sum_{n=0}^{2}\sum_{n'=0}^{2}\sigma_{\gamma_n^{(e)}\gamma_{n'}^{(e)}}^2\left(\frac{\partial f}{\partial \gamma_n^{(e)}}\right)\left(\frac{\partial f}{\partial \gamma_{n'}^{(e)}}\right) + \sum_{n=0}^{2}\sum_{n'=0}^{2}\sigma_{\gamma_n^{(p)}\gamma_{n'}^{(p)}}^2\left(\frac{\partial f}{\partial \gamma_n^{(p)}}\right)\left(\frac{\partial f}{\partial \gamma_{n'}^{(p)}}\right) + \sigma_{p_{m,ref}^{(e)}}^2\left(\frac{\partial f}{\partial p_{m,ref}^{(e)}}\right) + \sigma_{p_{m,ref}^{(p)}}^2\left(\frac{\partial f}{\partial p_{m,ref}^{(p)}}\right)$$

$$+ \sigma_{p_{m,0}^{(EUV)}}^2\left(\frac{\partial f}{\partial p_{m,0}^{(EUV)}}\right)^2 + \sigma_{\rho_e}^2\left(\frac{\partial f}{\partial \rho_e}\right)^2 + \sigma_{\rho_p}^2\left(\frac{\partial f}{\partial \rho_p}\right)^2 + \sigma_{z_\alpha}^2\left(\frac{\partial f}{\partial z_\alpha}\right)^2 + \sigma_{\alpha_0}^2\left(\frac{\partial f}{\partial \alpha_0}\right)^2 + \sigma_{H_\alpha}^2\left(\frac{\partial f}{\partial H_\alpha}\right)^2$$

29

Explicit expressions for each of these derivatives are given below. In most cases, the parameters appear in only a few terms, so that the individual partial derivatives are relatively simple. Since it is essential to the $h_m E$ error propagation analysis, the partial derivative of $p_i = \sum p_i^{(b)}$ will be evaluated first.

$$\frac{\partial p_i}{\partial h_m E} = \frac{\partial p_i}{\partial z}\bigg|_{z=h_m E} = \sum_b Q_b p_m^{(b)} \frac{\partial}{\partial u_b} S(u_b, \psi_b) \frac{\partial u_b}{\partial z}\bigg|_{z=h_m E} \tag{A10}$$

where, as usual, $\psi_b = 0$ for $b = e$ or p, and $\psi_{EUV} = \chi$. Evaluating the derivative of S yields

$$\frac{\partial}{\partial u} S(u, \psi) = \left[e^{-u} Ch(\psi) - 1\right] S(u, \psi) \tag{A11}$$

which appears in most of the partial derivatives that must be evaluated. Also important is the partial derivative of $\partial p_i / \partial z$:

$$\frac{\partial}{\partial h_m E}\left[\frac{\partial p_i}{\partial z}\bigg|_{z=h_m E}\right] = \frac{\partial^2 p_i}{\partial z^2}\bigg|_{z=h_m E} = \sum_b Q_b p_m^{(b)} \frac{\partial^2}{\partial u_b^2} S(u_b, \psi) \frac{\partial u_b}{\partial z}\bigg|_{z=h_m E} \tag{A12}$$

which requires the evaluation of $\partial^2 S / \partial u^2$:

$$\frac{\partial^2 S}{\partial u^2} = \left[e^{-2u} Ch^2(\psi) - 3e^{-u} Ch(\psi) + 1\right] S(u, \psi) \tag{A13}$$

The general expressions for $\dfrac{\partial h_m E}{\partial b_k}$ and $\dfrac{\partial N_m E}{\partial b_k}$ are given by Equations (A6) and (A8) above. The expressions are in terms of partial derivatives of p_i with respect to b_k, which may represent either an argument or a parameter. It is these partial derivatives that are evaluated below.

NOTE: In both Equations (A6) and (A8), the dependence on $h_m E$ is taken into account explicitly, so in deriving the following expressions p_i was treated as a function of z while the argument and parameter derivatives were taken, and then the result was evaluated at $z = h_m E$.

We begin by evaluating the partial derivatives of p_i and $\partial p_i / \partial z$ with respect to the five relevant arguments (errors in χ being ignored):

Q_b:
$$\frac{\partial p_i}{\partial Q_b} = p_m^{(b)} S(u_b, \psi), \qquad b = e, p, EUV \tag{A14}$$

$$\frac{\partial}{\partial Q_b}\left(\frac{\partial p_i}{\partial z}\right) = p_m^{(b)}\left[e^{-u} Ch(\psi) - 1\right] S(u, \psi), \qquad b = e, p, EUV \tag{A15}$$

$$E_{0,b}: \qquad \frac{\partial p_i}{\partial E_{0,b}} = Q_b \left\{ \frac{\partial p_m^{(b)}}{\partial E_{0,b}} + p_m^{(b)} \left[e^{-u_b} - 1 \right] \frac{\partial u_b}{\partial E_{0,b}} \right\} S(u_b, 0), \qquad b = e, p \qquad \text{(A16)}$$

$$\frac{\partial}{\partial E_{0,b}} \left(\frac{\partial p_i}{\partial z} \right) = Q_b \left\{ \frac{\partial p_m^{(b)}}{\partial E_{0,b}} \left[e^{-u_b} - 1 \right] + \left[e^{-2u_b} - 3e^{-u_b} + 1 \right] \frac{\partial u_b}{\partial E_{0,b}} \right\} S(u_b, 0), \qquad b = p, e \qquad \text{(A17)}$$

where

$$\frac{\partial u_b}{\partial E_{0,b}} = \frac{H_b \left[-\frac{\partial h_m^{(b)}}{\partial E_{0,b}} \right] - \left[z - h_m^{(b)} \right] \frac{\partial H_b}{\partial E_{0,b}}}{H_b^2}, \qquad b = e, p \qquad \text{(A18)}$$

Explicitly

$$\frac{\partial h_m^{(b)}}{\partial E_{0,b}} = -\sum_{n=1}^{3} n \beta_n^{(b)} \left[\frac{1}{E_{0,b}} \right]^{n+1}, \qquad b = e, p \qquad \text{(A19)}$$

$$\frac{\partial p_m^{(b)}}{\partial E_{0,b}} = p_m^{(b)} \left[\gamma_0^{(b)} \ln 10 + \left(\gamma_1^{(b)} + 2\gamma_2^{(b)} \log_{10} E_{0,b} \right) \frac{1}{E_{0,b}} \right], \qquad b = e, p \qquad \text{(A20)}$$

$$\frac{\partial H_b}{\partial E_{0,b}} = -\frac{\rho_b}{e \left[p_m^{(b)} \right]^2} \frac{\partial p_m^{(b)}}{\partial E_{0,b}}, \qquad b = e, p \qquad \text{(A21)}$$

Now we produce the derivatives with respect to the parameters

$$\beta_n^{(b)}: \qquad \frac{\partial p_i}{\partial \beta_n^{(b)}} = Q_b p_m^{(b)} \left[e^{-u_b} - 1 \right] S(u_b, 0) \frac{\partial u_b}{\partial h_m^{(b)}} \frac{\partial h_m}{\partial \beta_n^{(b)}}, \qquad b = e, p \qquad \text{(A22)}$$

or

$$\frac{\partial p_i}{\partial \beta_n^{(b)}} = -Q_b \frac{p_m^{(b)}}{H_b} \left[e^{-u_b} - 1 \right] S(u_b, 0) \left[\frac{1}{E_{0,b}} \right]^n, \qquad b = e, p \qquad \text{(A23)}$$

Similarly

$$\frac{\partial}{\partial \beta_n^{(b)}}\left(\frac{\partial p_i}{\partial z}\right) = -Q_b\left[e^{-2u_b} - 3e^{-u_b} + 1\right]\frac{p_i^{(b)}}{H_b^2}\left[\frac{1}{E_{0,b}}\right]^n, \qquad b = e, p \tag{A24}$$

---

h_0:
$$\frac{\partial p_i}{\partial h_0} = -\left[e^{-u_{EUV}}\,\mathrm{Ch}(\chi) - 1\right]\frac{p_m^{(EUV)}}{H_n} \tag{A25}$$

$$\frac{\partial}{\partial h_0}\left(\frac{\partial p_i}{\partial z}\right) = -\frac{1}{H_n^2}\left[e^{-2u_{EUV}}\,\mathrm{Ch}^2(\chi) - 3e^{-u_{EUV}}\,\mathrm{Ch}(\chi) + 1\right]p_i^{(EUV)} \tag{A26}$$

H_n:
$$\frac{\partial p_i}{\partial H_n} = -\frac{u_{EUV}}{H_n}\left[e^{-u_{EUV}}\,\mathrm{Ch}(\chi) - 1\right]p_i^{(EUV)} \tag{A27}$$

$$\frac{\partial}{\partial H_n}\left(\frac{\partial p_i}{\partial z}\right) = -\frac{u_{EUV}}{H_n^2}\left[e^{-2u_{EUV}}\,\mathrm{Ch}^2(\chi) - 3e^{-u_{EUV}}\,\mathrm{Ch}(\chi) + 1\right]p_i^{(EUV)} \tag{A28}$$

$\gamma_n^{(b)}$:
$$\frac{\partial p_i}{\partial \gamma_n^{(b)}} = Q_b\frac{\partial p_m^{(b)}}{\partial \gamma_n^{(b)}}S(u_b, 0) + Q_b p_m^{(b)}\frac{\partial S}{\partial u_b}\frac{\partial u_b}{\partial H_b}\frac{\partial H_b}{\partial p_m^{(b)}}\frac{\partial p_m^{(b)}}{\partial \gamma_n^{(b)}}, \qquad b = e, p \tag{A29}$$

Since

$$\frac{\partial p_m^{(b)}}{\partial \gamma_n^{(b)}} = p_m^{(b)}\left[\log_{10}\left(\frac{E_{0,b}}{E_{ref}^{(b)}}\right)\right]^n \ln 10 \tag{A30}$$

and since $\dfrac{\partial u_b}{\partial H_b} = -\dfrac{u_b}{H_b}$ and $\dfrac{\partial H_b}{\partial p_m^{(b)}} = -\dfrac{H_b}{p_m^{(b)}}$, we have

$$\frac{\partial p_i}{\partial \gamma_n^{(b)}} = \left[1 + \left(e^{-u_b} - 1\right)u_b\right]p_i^{(b)}\left[\log_{10}\left(\frac{E_{0,b}}{E_{ref}^{(b)}}\right)\right]^n \ln 10 \tag{A31}$$

Similarly

$$\frac{\partial}{\partial \gamma_n^{(b)}}\left(\frac{\partial p_i}{\partial z}\right) = \left[u_b e^{-2u_b} + (1 - 3u_b)e^{-u_b} - 1 + u_b\right]\frac{p_i^{(b)}}{H_b}\left[\log_{10}\left(\frac{E_{0,b}}{E_{ref}^{(b)}}\right)\right]^n \ln 10, \qquad b = e, p \tag{A32}$$

$p_m^{(b)}\left(E_{ref}^{(b)}\right)$:
$$\frac{\partial p_i}{\partial p_m^{(b)}\left(E_{ref}^{(b)}\right)} = \frac{p_m^{(b)}\left(E_{0,b}\right)}{p_m^{(b)}\left(E_{ref}^{(b)}\right)}, \qquad b = e, p \tag{A33}$$

32

$$\frac{\partial}{\partial p_m^{(b)}\left(E_{ref}^{(b)}\right)}\left(\frac{\partial p_i}{\partial z}\right) = \frac{1}{p_m^{(b)}\left(E_{ref}^{(b)}\right)}\frac{\partial p_i^{(b)}}{\partial z}, \qquad b = e,p \tag{A34}$$

with $E_{ref}^{(e)} = 1$ keV and $E_{ref}^{(p)} = 8$ keV.

$p_m^{(EUV)}(0)$:
$$\frac{\partial p_i}{\partial p_m^{(EUV)}(0)} = \frac{p_i^{(EUV)}(\chi)}{p_m^{(EUV)}(0)} = Q_{EUV}S(u_{EUV},\chi) \tag{A35}$$

$$\frac{\partial}{\partial p_i^{(EUV)}(0)}\left(\frac{\partial p_i}{\partial z}\right) = \frac{1}{p_i^{(EUV)}(0)}\frac{\partial p_i^{(EUV)}}{\partial z} \tag{A36}$$

ρ_b:
$$\frac{\partial p_i}{\partial \rho_b} = Q_b p_m^{(b)}\frac{\partial S}{\partial u_b}\frac{\partial u_b}{\partial H_b}\frac{\partial H_b}{\partial \rho_b} = -Q_b p_m^{(b)}\frac{u_b}{\rho_b}\left[e^{-u_b}-1\right]S(u_b,0), \qquad b = e,p \tag{A37}$$

$$\frac{\partial}{\partial \rho_b}\left(\frac{\partial p_i}{\partial z}\right) = -Q_b \frac{p_m^{(b)}}{H_b}\frac{\partial^2 S}{\partial u_b^2}\frac{\partial u_b}{\partial H_b}\frac{\partial H_b}{\partial \rho_b} = Q_b \frac{p_m^{(b)}}{H_b}\frac{u_b}{\rho_b}\left[e^{-2u_b}-3e^{-u_b}+1\right]S(u_b,0), \qquad b = e,p \tag{A38}$$

While $\dfrac{\partial p_i}{\partial \alpha_0} = \dfrac{\partial}{\partial \alpha_0}\left(\dfrac{\partial p_i}{\partial z}\right) = 0$ and $\dfrac{\partial p_i}{\partial H_\alpha} = \dfrac{\partial}{\partial H_\alpha}\left(\dfrac{\partial p_i}{\partial z}\right) = 0$, both $h_m E$ and $N_m E$ are explicitly dependent on $\alpha(z)$ so

$$\frac{\partial h_m E}{\partial z_\alpha} = \frac{\partial h_m E}{\partial \alpha_0} = 0 \tag{A39}$$

$$\frac{\partial h_m E}{\partial H_\alpha} = \begin{cases} 0, & z \leq z_\alpha \\[2ex] \dfrac{1}{\left[\left.\dfrac{\partial^2 p_i}{\partial z^2}\right|_{z=h_m E} + \dfrac{1}{H_\alpha}\left.\dfrac{\partial p_i}{\partial z}\right|_{z=h_m E}\right]}\dfrac{p_i}{H_\alpha^2}, & z > z_\alpha \end{cases} \tag{A40}$$

$$\frac{\partial N_m E}{\partial z_\alpha} = -\frac{p_i}{\alpha H_\alpha} \tag{A41}$$

$$\frac{\partial N_m E}{\partial \alpha_0} = -\frac{N_m E}{2\alpha_0} \tag{A42}$$

$$\frac{\partial N_m E}{\partial H_\alpha} = \frac{1}{2}\frac{h_m E - z_\alpha}{H_\alpha^2}N_m E \tag{A43}$$